

Supporting information

## Derivations of CAH CFE FEB and $W_a$ based on a dynamic equation

### 1. Establishment of a dynamic equation

Fig. 1 (see Fig. 1 in the original) shows changes of droplet states on superhydrophobic surfaces (SHS) while water is added and withdrawn.

**Fig. 1a**, area of spherical cap (given  $R_1$  of a droplet radius) in the initial state

$$S_1 = 2\pi R_1 h_1 = 2\pi R_1 (R_1 - r_1 \text{ctg} \theta_w) = 2\pi R_1^2 (1 - \cos \theta_w) \quad (1)$$

**Fig. 1b**, area of spherical cap in the pre-advancing state

$$S_2 = 2\pi R_2 h_2 = 2\pi R_1^2 \left( \frac{\sin \theta_w}{\sin \theta_a} \right)^2 (1 - \cos \theta_a) > S_1 \quad (2)$$

Volume of spherical segment

$$V_2 = \frac{1}{6} \pi h_2 (3r_2^2 + h_2^2) = \frac{1}{6} \pi R_1^3 (\sin^3 \theta_w) \left[ 3 + (\csc \theta_a - \text{ctg} \theta_a)^2 \right] (\csc \theta_a - \text{ctg} \theta_a) \quad (3)$$

**Fig. 1c**, Volume of spherical segment in the advancing state

$$V_3 = \frac{1}{6} \pi h_3 (3r_3^2 + h_3^2) = \frac{1}{6} \pi R_3^3 (1 - \cos \theta_w) \left[ 3 \sin^2 \theta_w + (1 - \cos \theta_w)^2 \right] \quad (4)$$

Based on  $V_3 = V_2$ , solving equation

$$\frac{1}{6} \pi R_3^3 (1 - \cos \theta_w) \left[ 3 \sin^2 \theta_w + (1 - \cos \theta_w)^2 \right] = \frac{1}{6} \pi R_1^3 (\sin^3 \theta_w) \left[ 3 + (\csc \theta_a - \text{ctg} \theta_a)^2 \right] (\csc \theta_a - \text{ctg} \theta_a) \quad \text{for}$$

$$R_3 = \sqrt[3]{\left[ \left( 3 + \text{tg}^2 \frac{\theta_a}{2} \right) \text{tg} \frac{\theta_a}{2} \right] / \left[ \left( 3 + \text{tg}^2 \frac{\theta_w}{2} \right) \text{tg} \frac{\theta_w}{2} \right]} R_1 \quad (5)$$

Consequently, area of spherical cap

$$S_3 = 2\pi R_3 h_3 = 2\pi R_3^2 (1 - \cos \theta_w) = 4\pi \sin^2 \frac{\theta_w}{2} \sqrt[3]{\left[ \left( 3 + \text{tg}^2 \frac{\theta_a}{2} \right) \text{tg} \frac{\theta_a}{2} \right] / \left[ \left( 3 + \text{tg}^2 \frac{\theta_w}{2} \right) \text{tg} \frac{\theta_w}{2} \right]}^2 R_1^2 \quad (6)$$

Among it, radius of three-phase contact line

$$r_3 = R_3 \sin \theta_w = \sqrt[3]{\left[\left(3 + \operatorname{tg}^2 \frac{\theta_a}{2}\right) \operatorname{tg} \frac{\theta_a}{2}\right] / \left[\left(3 + \operatorname{tg}^2 \frac{\theta_w}{2}\right) \operatorname{tg} \frac{\theta_w}{2}\right]} r_1 \quad (7)$$

For receding (Fig. 1a–1c'), following the same method, we may find the similar quantities:

$$r_3' = R_3' \sin \theta_w = \sqrt[3]{\left[\left(3 + \operatorname{tg}^2 \frac{\theta_r}{2}\right) \operatorname{tg} \frac{\theta_r}{2}\right] / \left[\left(3 + \operatorname{tg}^2 \frac{\theta_w}{2}\right) \operatorname{tg} \frac{\theta_w}{2}\right]} r_1 \quad (8)$$

For the SHS, generally speaking, there is a relation:

$$\theta_a > \theta_w > \theta_r > 150^\circ \quad (9)$$

Resultantly, we can find:

$$\operatorname{tg}^2 \frac{\theta_a}{2} \gg 3, \quad \operatorname{tg}^2 \frac{\theta_r}{2} \gg 3, \quad \operatorname{tg}^2 \frac{\theta_w}{2} \gg 3 \quad (10)$$

Based on Eq. (10), Eqs. (7) and (8) may be simplified into Eqs. (11) and (12), respectively.

$$r_3/r_1 \approx \left(\operatorname{tg} \frac{\theta_a}{2} / \operatorname{tg} \frac{\theta_w}{2}\right) (= q_a) \quad (11)$$

$$r_3'/r_1 \approx \left(\operatorname{tg} \frac{\theta_r}{2} / \operatorname{tg} \frac{\theta_w}{2}\right) (= q_r) \quad (12)$$

According to the regulation for SHS, static apparent CA ( $\theta_w$ )  $> 150^\circ$ , sliding angle (SA)  $< 5^\circ$ . In view of  $\theta_w$  hard larger than  $170^\circ$  in most cases, let  $\theta_w$  range from  $155^\circ$  to  $170^\circ$ . According to Eqs. (11) and (12) common ratios  $q_a$  and  $q_r$  may be found by numerical calculations.

$$\text{Let } q_{aji} = \frac{r_3}{r_1} = \frac{\operatorname{tg} \frac{(\theta_w + i)}{2}}{\operatorname{tg} \frac{\theta_w}{2}} = \frac{\operatorname{tg} [(77 + j) + i/2]}{\operatorname{tg} (77 + j)} \quad (13)$$

$$q_{rjk} = \frac{r_3'}{r_1} = \frac{\operatorname{tg} \frac{(\theta_w - k)}{2}}{\operatorname{tg} \frac{\theta_w}{2}} = \frac{\operatorname{tg} [(77 + j) - k/2]}{\operatorname{tg} (77 + j)} \quad (1 \leq j \leq 8, j \in N, i = 1, 2 \text{ or } 3, k = 1, 2 \text{ or } 3) \quad (14)$$

As Fig. 2 shows, both  $q_a$  and  $q_r$  may be approximately simplified for the

corresponding average  $c_a = \frac{1}{24} \sum_{j=1}^8 \sum_{i=1}^3 q_{aji} = 1.15$ ,  $c_r = \frac{1}{24} \sum_{j=1}^8 \sum_{k=1}^3 q_{rjk} = 0.89$ , respectively (both  $i$  and  $k$  denote increment of  $\theta_a$  and  $\theta_r$  relative to  $\theta_w$ , respectively, but  $i$  is not always equal to  $k$ ,  $j$  denotes increment of half of  $\theta_w$  relative to  $77^\circ$ ), because there are only a few hundredths errors between  $q_{aji}$  and  $c_a$  or  $q_{rjk}$  and  $c_r$  in most cases. Moreover, due to half of  $\theta_w$  larger  $75^\circ$ , then  $\text{tg} \frac{\theta_w}{2} > \frac{\theta_w}{2} > 3.7$ , this can improve accuracy of calculations of  $\theta_a, \theta_r$  and  $CAH$  significantly according to Eqs. (11)–(14).

By doing so, Eqs. (17) and (18) may be finally simplified,

$$\left( \text{tg} \frac{\theta_a}{2} / \text{tg} \frac{\theta_w}{2} \right) = c_a = 1.15 \quad (15)$$

$$\left( \text{tg} \frac{\theta_r}{2} / \text{tg} \frac{\theta_w}{2} \right) = c_r = 0.89 \quad (16)$$

These are so-called dynamic equations which describe relationships between advancing and receding CAs ( $\theta_a, \theta_r$ ) and the static apparent CAs ( $\theta_w$ ). Certainly, both  $c_a$  and  $c_r$  are only applied to the calculations of property parameters of the SHSs, i.e.,  $\theta_a, \theta_r, CAH, CFE, FEB$  and  $W_a$ . If both  $c_a$  and  $c_r$  are used in some non-superhydrophobic states, it is no more than used for design and datum analysis rather than theory proving. Otherwise, it appears to be mistakes of circular reasoning. Actually common ratios  $q_a$  and  $q_r$  may be also determined by curve-fitting as a function of the apparent CAs ( $q_a = f(\theta_w)$  or  $q_r = g(\theta_w)$ ), which seems to be more exact. However, it will bring the relevant calculations unnecessary complexity with results not being satisfactory.

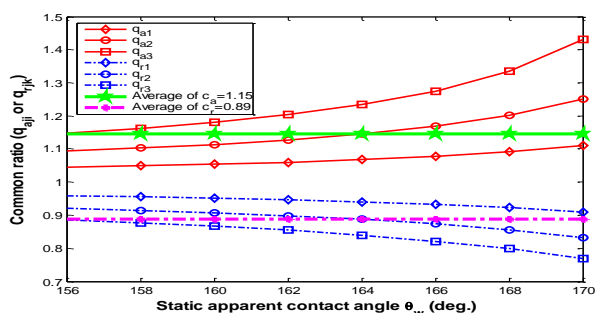


**Fig. 2** Numerical calculation of  $q_a$  (or  $c_a$ ),  $q_r$  (or  $c_r$ ).

## 2. Determination of contact angle hysteresis (CAH)

According to Eqs. (15) and (16), CAH as well as  $\theta_a, \theta_r$  (known  $\theta_w$ ) can be found,

$$\left. \begin{aligned} c_a &= \operatorname{tg} \frac{\theta_a}{2} / \operatorname{tg} \frac{\theta_w}{2} \Rightarrow \theta_a = 2 * \operatorname{arctg} \left( c_a \operatorname{tg} \frac{\theta_w}{2} \right) \\ c_r &= \operatorname{tg} \frac{\theta_r}{2} / \operatorname{tg} \frac{\theta_w}{2} \Rightarrow \theta_r = 2 * \operatorname{arctg} \left( c_r \operatorname{tg} \frac{\theta_w}{2} \right) \end{aligned} \right\} \quad (17)$$

$$\text{CAH} = \theta_a - \theta_r = 2 \left[ \operatorname{arctg} (1.15\xi) - \operatorname{arctg} (0.89\xi) \right] \quad \left( \xi = \operatorname{tg} \frac{\theta_w}{2} \right) \quad (18)$$

## 3. Determination of changes in free energy (CFE)

From Fig. 1a to 1b (advancing), because three-phase contact line does not move (Fig. 1e), the CFE, which is defined as difference of liquid-gas interfacial free energy between the pre-advancing and the initial states, only depends on liquid-gas interfaces, and can be found in simple,

$$\Delta E_{aw} = E_2 - E_1 = (S_2 - S_1) \gamma^{la} = s_0 \gamma^{la} \left( \sec^2 \frac{\theta_a}{2} - \sec^2 \frac{\theta_w}{2} \right) = s_0 \gamma^{la} \beta(\theta) \Big|_{\theta_w}^{\theta_a} \quad (19)$$

where  $s_0 = \pi R_1^2 \sin^2 \theta_w$ ,  $\beta(\theta) = \sec^2 \frac{\theta}{2}$  (20)

Similarly, from Fig. 1a to 1c' (receding), the CFE may be also determined,

$$\Delta E_{rw} = s_0 \gamma^{la} \left( \sec^2 \frac{\theta}{2} \right) \Big|_{\theta_w}^{\theta_r} = s_0 \gamma^{la} \beta(\theta) \Big|_{\theta_w}^{\theta_r} \quad (21)$$

where  $\theta_w$  and  $\beta(\theta)$  are defined as equilibrium apparent CA, and CAH factor which shows the contribution of  $\theta$  to CFE (see Fig. 2 in original), respectively.

For the SHS, considering less CAH ( $CAH < 10^\circ$ ) and less effect of large droplet volume on CA,<sup>1</sup> and integrating advancing with receding, by analogy we can find the CFE associated with CAH:

$$\Delta E_{ar} = E_2 - E_2' = (S_2 - S_2') \gamma^{la} = \gamma^{la} \beta_0(\theta) \Big|_{\theta_1}^{\theta_2} \quad (22)$$

#### 4. Determination of free energy barrier (FEB)

From Fig. 1b to 1c, because three-phase contact line is moved away (Fig. 1f), the normalized advancing free energy barrier with respect to  $\gamma^{la}$ , defined as the difference of interfacial FE between pre-advancing and advancing states at constant volume, mainly depends on liquid-gas, liquid-solid, and solid-gas interfaces. Especially, it is completely different from the local free energy barriers only based on the 2-D model.<sup>2-4</sup> Conversely,  $F^{aw}/\gamma^{la}$  (including both  $F^{rw}/\gamma^{la}$  and  $F^{ar}/\gamma^{la}$ ) here is the average obstacle relating to a 3-D droplet in macro-scale rather than in micro-scale or at the local point/line. Therefore, it does not involve the intermediate process (these have been done in our previous study),<sup>3,5-8</sup> let alone metastable states. In fact, the average values has more practical significance than the local values, because experiment values of some quantities, e.g., CA, CAH, all belong to the average values, as both Wenzel's and Cassie-Baxter's equations are based on the averages. Local values are only applied to theoretical analysis.

$$\begin{aligned} \Delta F^{aw} = F_2 - F_3 &= \left[ s \gamma^{lg} + \pi Y r^2 \gamma^{ls} + \pi Y (r^2 - r_3^2) \gamma^{lg} \right] - \left[ s \gamma^{lg} + \pi Y r^2 \gamma^{ls} \right] \\ \Rightarrow \frac{\Delta F^{aw}}{\gamma^{la}} &= 4\pi R_1^2 \cos^2 \frac{\theta_w}{2} \left( \operatorname{tg} \frac{\theta_w}{2} - \operatorname{tg} \frac{\theta_a}{2} \right) \left[ \operatorname{tg} \frac{\theta_a}{2} - \cos \theta_w \left( \operatorname{tg} \frac{\theta_w}{2} + \operatorname{tg} \frac{\theta_a}{2} \right) \right] \cos \frac{\theta_w}{2} \end{aligned} \quad (23)$$

where  $Y$  denotes surface roughness ratio.

Similarly, receding FEB may be found:

$$\begin{aligned} \Delta F^{rw} &= F_2' - F_3' = [s_2' \gamma^{la} + \pi Y r_2'^2 \gamma^{sl}] - [s_3' \gamma^{la} + \pi Y r_3'^2 \gamma^{sl} + \pi Y (r_3'^2 - r_2'^2) \gamma^{sa}] \\ \Rightarrow \frac{\Delta F^{rw}}{\gamma^{la}} &= 4\pi R_1^2 \cos^2 \frac{\theta_w}{2} \left( \operatorname{tg} \frac{\theta_w}{2} - \operatorname{tg} \frac{\theta_r}{2} \right) \left[ \operatorname{tg} \frac{\theta_r}{2} - \cos \theta_w \left( \operatorname{tg} \frac{\theta_w}{2} + \operatorname{tg} \frac{\theta_r}{2} \right) \cos^2 \frac{\theta_w}{2} \right] \end{aligned} \quad (24)$$

For the whole hysteresis process, a droplet must synchronously overcome the advancing and receding free energy barriers. Therefore, the FEB corresponding to CAH may be defined:

$$\begin{aligned} \frac{\Delta F^{ar}}{\gamma^{la}} &= \left\| \frac{\Delta F^{aw}}{\gamma^{la}} \right\| - \left\| \frac{\Delta F^{rw}}{\gamma^{la}} \right\| \\ &= 4\pi R_1^2 \cos^2 \frac{\theta_w}{2} \left[ \cos \theta_w \cos^2 \frac{\theta_w}{2} \left( \operatorname{tg}^2 \frac{\theta_a}{2} + \operatorname{tg}^2 \frac{\theta_r}{2} - 2 \operatorname{tg}^2 \frac{\theta_w}{2} \right) + \operatorname{tg} \frac{\theta_w}{2} \left( \operatorname{tg} \frac{\theta_a}{2} + \operatorname{tg} \frac{\theta_r}{2} \right) - \left( \operatorname{tg}^2 \frac{\theta_a}{2} + \operatorname{tg}^2 \frac{\theta_r}{2} \right) \right] \end{aligned} \quad (25)$$

Significantly, in spite of the unequal mass of the droplet in the advancing and receding states due to the added or withdrawn droplet, this does not affect calculations of the FEBs, because Eqs. (19)–(25) show that CFE and FEB only depend on the apparent CAs  $(\theta_a, \theta_r, \theta_w)$  at a given  $R_1$ .

### 5. Determination of normalized adhesion work ( $W_a$ ) and spreading coefficient ( $S_{L/S}$ )

When a droplet is dropped onto SHS, the droplet bedews it (Fig.1a). Because of constant temperature and pressure, we can find the changes in Gibbs free energy or adhesion work per unit area,

$$w_a = -\Delta G = -(\gamma^{sl} - \gamma^{sa} - \gamma^{la}) \quad (26)$$

According to Young's equation, simplify it again,

$$w_a = -\Delta G = \gamma^{la} (1 + \cos \theta_w) \quad (27)$$

Consequently, the total adhesion work of the solid–liquid interface may be found and normalized,

$$W_a = \Delta F^{ls} / \gamma^{la} = (1 + \cos \theta_w) \times \pi \times (R_1 \sin \theta_w)^2 \quad (28)$$

Meanwhile, we also may think that the droplet automatically spreads to form a very

much limited solid–liquid interface (Fig.1a). The changes in Gibbs free energy or spreading coefficient per unit area may be determined,

$$S_{L/S} = -\Delta G = (\gamma^{sa} - \gamma^{sl} - \gamma^{la}) = w_a - w_c \quad (w_a = \gamma^{sa} + \gamma^{la} - \gamma^{sl}, \quad w_c = 2\gamma^{la}) \quad (29)$$

Referring to Young's equation, the above equations may be simplified,

$$S_{L/S} = -\Delta G = (\gamma^{sa} - \gamma^{sl} - \gamma^{la}) = \gamma^{la} (\cos \theta_w - 1) \quad (30)$$

For the SHS,  $S_{L/S} < 0$  due to  $\theta_w > 150^\circ$ . A water droplet is hard to spread. How to technically decrease or increase  $S_{L/S}$  is of considerable importance to a number of industrial applications.

## References

- 1 A. Marmur, J. Colloid Interface Sci., 1994, **168**(1), 40.
- 2 A. Marmur, *Adv. Colloid Interface Sci.*, 1994, **50**, 121.
- 3 W. Li, A. Amfirazli, J. Colloid Interface Sci., 2005, **292**(1), 195.
- 4 R. E. Johnson Jr., R. H. Dettre, *Adv. Chem. Ser.*, 1964, **43**, 112.
- 5 H. Y. Zhang, W. Li, G. P. Fang, *Appl. Surf. Sci.*, 2012, **258**, 2707.
- 6 H. H. Liu, H. Y. Zhang, W. Li, *Langmuir*, 2011, **27**, 6260.
- 7 H. Y. Zhang, W. Li, Wen Li, Daoyi Cui, Zhiwei Hu, Liang Xu, *Colloids and Surfaces A: Physicochem. Eng. Aspects*, 2012, DOI:10.1016/j.colsurfa.2012.01.036.
- 8 W. Li, A. Amirfazli, *Adv. Colloid Interface Sci.*, 2007, **132**, 51.